

# Vision-Language Models can Identify Distracted Driver Behavior from Naturalistic Videos

Md Zahid Hasan, Jiajing Chen, Jiyang Wang, Ameya Joshi,  
Senem Velipasalar, Chinmay Hegde, Anuj Sharma, Soumik Sarkar

**Abstract**—Recognizing the activities, causing distraction, in real-world driving scenarios is critical for ensuring the safety and reliability of both drivers and pedestrians on the roadways. Conventional computer vision techniques are typically data-intensive and require a large volume of annotated training data to detect and classify various distracted driving behaviors, thereby limiting their efficiency and scalability. We aim to develop a generalized framework that showcases robust performance with access to limited or no annotated training data. Recently, vision-language models have offered large-scale visual-textual pretraining that can be adapted to task-specific learning like distracted driving activity recognition. Vision-language pretraining models, such as CLIP, have shown significant promise in learning natural language-guided visual representations. This paper proposes a CLIP-based driver activity recognition approach that identifies driver distraction from naturalistic driving images and videos. CLIP’s vision embedding offers zero-shot transfer and task-based finetuning, which can classify distracted activities from driving video data. Our results show that this framework offers state-of-the-art performance on zero-shot transfer and video-based CLIP for predicting the driver’s state on two public datasets. We propose both frame-based and video-based frameworks developed on top of the CLIP’s visual representation for distracted driving detection and classification task and report the results. Our code is available at <https://github.com/zahid-isu/DriveCLIP>

**Index Terms**—Distracted driving, Computer vision, CLIP, Vision-language model, Zero-shot transfer, Embedding

## I. INTRODUCTION

**D**istracted driving accounts for almost 10% of all fatalities on U.S. roads. Although cell phone usage is often synonymous with distracted driving, the problem is broader. The Center for Disease Control and Prevention (CDC) identifies three forms of distraction: i) visual distraction, where the driver takes their eyes away from the road. This can be due to several reasons, such as looking at the GPS, Billboard, etc.; ii) manual distraction, where the driver takes their hands off of the steering wheel; and iii) cognitive distraction, where the driver takes their mind off the driving task, which can be due to

singing, talking, etc. The association of crashes with distracted behavior is underreported. Verifying the distraction in the post-crash investigation is difficult, and the driver at fault might not disclose this information voluntarily. Contrary to the numbers reported in crash analysis, Naturalistic Driving Data analysis by Dingus et al. [1] reported that almost 90% of their studied 905 crashes, which resulted in injury or property damage, can be attributed to driver-related factors (i.e., error, impairment, fatigue, and distraction). Naturalistic driving study (NDS) research involves observing drivers in real-world settings using unobtrusive instruments fitted to their vehicles. These studies cover drivers’ daily driving activity for a few months to years. With low-cost sensors and robust data handling infrastructure, NDS research is now easier to implement and has paved the way to comprehensively understanding the occurrence of driving events and driver responses in a natural environment. In most recent studies, such analysis has required humans to annotate driver distraction manually. The manual approach is useful but very time consuming and significantly increases the time of analysis. This study aims to reliably and efficiently identify distracted driving actions by drivers from naturalistic driving videos.

With the significant advances in deep learning and computer vision, there has been a considerable surge in video analytics for the classification of distracted driving. In recent studies, convolutional neural networks (CNN) have been widely employed for video-based distracted driving detection. For instance, Moslemi et al. [2] proposed a 3D CNN model for distracted driving detection using a dataset composed of videos captured in a naturalistic driving study. This model was designed to learn spatiotemporal features from video sequences, thus allowing it to capture not only the appearance of distracted behaviors but also their temporal dynamics. However, this type of model often requires large amounts of labeled training data, which is both time-consuming and costly to collect and annotate. Therefore, researchers have recently begun to investigate unsupervised and semi-supervised learning techniques. For instance, Xie et al. [3] introduced a semi-supervised learning method for distracted driving detection, wherein they combined labeled and unlabeled data to train their deep learning model.

The recent development of vision-language multimodal pretraining frameworks showcases promising potential across diverse applications. These pretraining frameworks employ a multi-modal contrastive-loss (see CLIP [4]), which paves the way for creating robust embeddings encompassing both text and vision tasks concurrently. This approach allowed several

M.Z. Hasan, A. Sharma, and S. Sarkar are with Iowa State University, Ames, IA-50010, e-mail: {zahid, anuj, soumik}@iastate.edu

J.Chen, J. Wang and S. Velipasalar are with the Department of Electrical Engineering and Computer Science, Syracuse University, Syracuse, NY-13244, e-mail: {jchen152, jwang127, svelipasg}@syr.edu

A. Joshi and C. Hegde are with the Department of Electrical and Computer Engineering, Brooklyn, NY-11201, e-mail: {ameya.joshi, chinmay.h}@nyu.edu

This material is based upon work supported by the Federal Highway Administration Exploratory Advanced Research Program under Agreement No. 693JJ31950022. Any opinions, findings, and conclusions or recommendations expressed in this publication are those of the Author(s) and do not necessarily reflect the view of the Federal Highway Administration.

Manuscript received May 31, 2023.

domains to use an almost zero-shot approach for tasks, such as object classification and object detection from images [4]–[7]. The study presented in this paper leverages CLIP’s vision and language embeddings for the specific task of distracted driving action recognition.

The task of distracted driving action recognition involves analyzing video data captured from a camera positioned inside the car, which records extensive time frames of driver behavior. The goal is to utilize this video data to determine whether the driver is distracted. Intuitively, one might consider training a video-text model from the ground up for this task. However, directly training such a model is impractical due to the need for large-scale video-text training data and considerable GPU resources. A more viable approach is to adapt pre-existing language-image models to the video domain. In fact, several recent studies have investigated strategies for transferring knowledge from these pretrained language-image models to other downstream tasks [6], [8]–[11].

Our proposed method benefits from key aspects of the pretrained CLIP model [4] and provides two main advantages. The first advantage is its ability to utilize zero-shot transfer, obviating the need for intensive training. This feature enhances scalability and feasibility, as it allows for a natural language-supervised understanding of video activities rather than relying exclusively on traditional supervised approaches. Unlike conventional computer vision methods, which tend to memorize human-annotated labels or features often found non-transferable, this model generally exhibits superior performance across diverse datasets rather than being constrained to a specific dataset. The second advantage of the proposed method is the potential to further finetune the visual representation with minimal annotations and training, thereby enhancing the overall performance of the system.

In summary, the key contributions of this work include the following:

- 1) We introduce and explore the performance of various vision-language-based frameworks (adapted from [4]) for the task of distracted driving action recognition with minimum training and during real-world driving scenarios.
- 2) We present both frame-based and video-based CLIP models and show that the inclusion of temporal information to the existing vision-language models offers superior performance on several distracted driving datasets. Moreover, we implement an in-depth analysis of model performance across different datasets and various experimental settings.
- 3) We study the robustness of our proposed frameworks in handling reduced training dataset size without compromising its performance, thus showcasing the model’s strong generalization capabilities. This signifies the potential for deploying these models in real-world scenarios where training data may be limited.

In this study, we have developed and tested four unique frameworks that are tailored specifically for analyzing distracted driving behavior. These frameworks include both frame-based and video-based models. The rest of this paper is organized as follows: Section II provides a review of

relevant research on distracted driving action recognition, highlighting key contributions as well as gaps that our study aims to address. Section III introduces the details of our methods. Section IV provides details about the datasets and the experimental setup for each framework. Section V presents the results of the performance evaluation of the proposed frameworks, performance comparison with existing models for distracted driving, an investigation into the impact of different real-world settings on the model performance and an ablation study. The paper is concluded in Section VI.

## II. RELATED WORK

In recent years, the area of driver action recognition and behavior analysis has attracted significant research interest. Various methods have been proposed, including several that use low-level hand-crafted feature engineering techniques. Techniques such as Cuboids [12], 3DHOG [13], and Dense Trajectories [14], [15] have been utilized to capture the temporal elements in video data. However, it has been noted that many of these techniques, which are specifically tailored to certain datasets, lack broad applicability as they are not trained end-to-end on large-scale datasets, resulting in limited generalization capabilities.

Prior to the advent of transformer technology, a significant portion of the proposed methodologies depended on various Convolutional Neural Network (CNN) architectures [3], [16], [17] for extracting important features from video content. There were certain CNN-based frameworks that gathered features from facial recognition [18], optical flow [19], and body posture assessment [20] in order to analyze video activities. These models, however, have limited generalization ability and are prone to failure if the feature extraction process fails, as they concentrate exclusively on a single type of feature.

While 3D CNNs have the capability to understand temporal features from video sequences [21], [22], their use is often constrained by high computational demands and practical implementation challenges in the naturalistic video domain. An alternative technique that is commonly adopted involves ensembling multiple CNN networks [23], [24], such as ResNet50 [25], Vgg16 [16], Xception [26], and Inception-v3 [27], each serving as a unique feature extractor. These are then incorporated into a weighted ensemble to yield a comprehensive global feature.

In addition, there are methods that adopt feature-level fusion [28]–[30]. These methods separately learn from RGB appearance and time-based features and later combine the learned features. However, the landscape of video action recognition is increasingly being shaped by vision transformer (ViT)-based techniques [31]–[33], which have started to dominate in video action recognition recently.

While these models exhibit satisfactory results on standard datasets, their effectiveness is significantly tied to large-scale datasets which demand substantial efforts for data annotation. Additionally, the training of these models is often geared towards mapping predefined categories, which impedes their ability to learn adaptable visual features on new data. Therefore, rather than confining the learning to specific visual

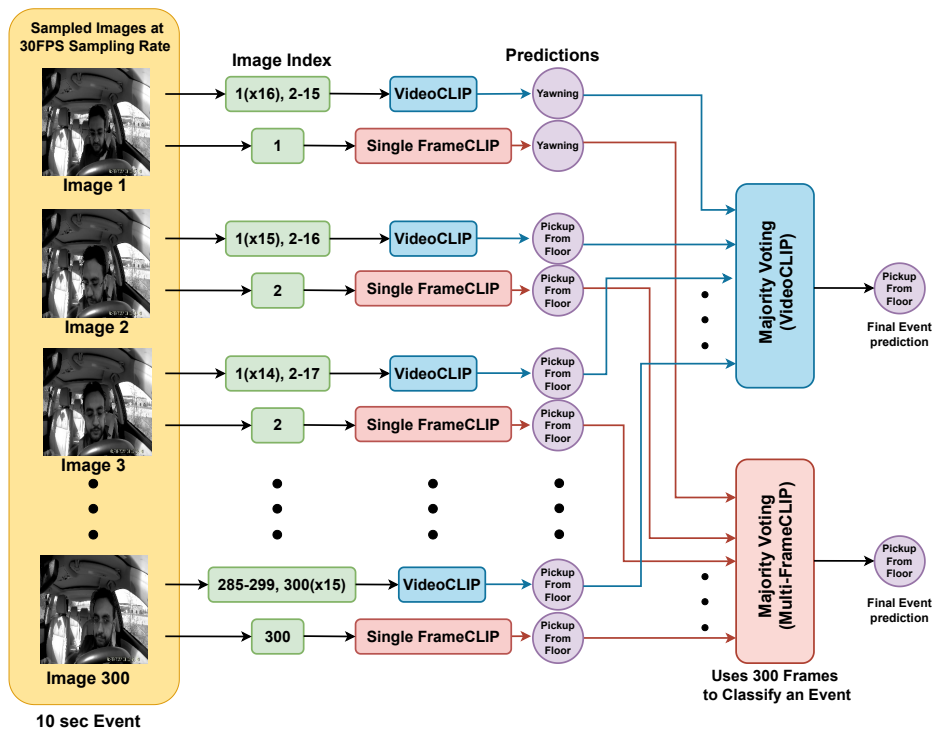


Fig. 1. An overview of the image-based and video-based CLIP frameworks. The yellow box shows the sampled frames from a 10-second event, i.e. a total of 300 frames at a rate of 30 frames per second. These frames are sampled from raw data (as depicted in Fig. 3). The VideoCLIP model uses 30 consecutive frames to form a short video clip as input, while the Single-frameCLIP model takes a single frame at a time. For the first sampled frame, the VideoCLIP generates a 30-frame video clip by repeating Image-1 sixteen times and including Images 2 to 15 (total 30 frames in the green box). The SingleframeCLIP model only uses Image-1 as its first input. This process continues for each subsequent frame. Finally, predictions for an entire event are made by calculating the majority vote from all individual frame predictions. Note that the Multi-frameCLIP applies majority voting on SingleframeCLIP’s predictions to get the final event prediction.

features within a single modality framework, learning from natural language supervision could provide increased adaptability and wider applicability.

The recent progress in vision-language pretraining approaches, including models like VideoCLIP [10] and ActionCLIP [6], has demonstrated improved performance in tasks related to video action recognition and understanding. These models were developed on a widely used vision-language model named CLIP model [4]. Miech et al. [34] introduce a large dataset, referred to as HowTo100M, for video-based CLIP training. Mithun et al. [35] propose a two-stage approach, which leverages web images and corresponding tags, along with fully annotated datasets, for learning the visual-semantic joint embedding. Dong et al. [36] attempt to solve the challenging problem of zero example video retrieval using textual features. Therefore, different methods have been developed to effectively learn from and utilize visual and textual data for tasks and visual-semantic joint embedding which underlines the potential of integrating visual and textual data in developing advanced models.

### III. METHODOLOGY

The primary objective of this work is to understand distracted driving behaviors captured from in-vehicle video footage and build an effective driver monitoring system. While distractions during driving can span a variety of situations, we predominantly focus on actions that distract the driver from the

primary task of safely operating the vehicle on the road, for instance talking on the phone, reaching behind, or drinking while driving. Visual data associated with distracted driving can present several complications in detecting distracted driving, including low-quality video data and the extensive human effort required to annotate videos for training supervised models. Furthermore, without a large volume of annotated visual data, training a high-performance supervised network is impossible. Therefore, we investigate to create a generalized framework that performs well without a strict reliance on labeled data or with only limited labeled data. To achieve this, we propose to leverage a contrastive vision-language pretraining framework designed to tackle these challenges with minimal annotated data. Moreover, we pay special attention to how our experiments were conducted, ensuring a robust and generalizable testing strategy. In real-world scenarios, the model will be expected to generalize its learning to new, never-before-seen drivers. Therefore, we always keep a unique set of driver samples separate for testing only. These drivers’ data is never presented to the model during its training phase, ensuring the model’s inferences during testing are made on fully unseen data. This strategy helps to strengthen the overall reliability of our model and its potential for successful real-world application.

### A. Overview of the Proposed Frameworks

We fundamentally propose two methodologies: (i) frame-based CLIP models (Zero-shotCLIP, Single-frameCLIP, and Multi-frameCLIP) and (ii) a video-based CLIP model (VideoCLIP). An overview of these frameworks is provided in Fig. 1. CLIP [4] is a popular vision-language model. It is proficient in most visual understanding tasks, since it was trained on a large variety (around 400 million) of image-text pairs from the web.

#### 1) Frame-based models

The frame-based models operate by taking inputs similar to the original CLIP model and making predictions on distracted actions. As shown in Fig. 2, the model projects the input image and text pairs into a multi-modal latent space and minimizes a contrastive loss, which enables it to learn meaningful and useful visual and textual representations that can be leveraged across different tasks. Therefore, the base model can be fine-tuned for task-specific learning. Given its ability to be instructed by natural language for a broad range of downstream tasks, such as video question answering and understanding actions from video, we develop our distracted driving analysis framework based on this model. A great advantage of using a pre-trained network over other strategies is the ability to utilize the pre-existing visual representation of the language prompt, offering the zero-shot transfer. In this work, we initially leverage CLIP’s pre-trained visual embedding for zero-shot transfer on distracted driving datasets, categorizing the distracted action classes without any additional training. Following this, we fine-tune a linear classifier layer built upon the original pre-trained CLIP model. The yellow block shown in Fig. 2 represents the frozen layers. We add the green block positioned on top of the yellow layers, which represents the trainable layer. This task-based, fine-tuning green block involves training a straightforward classifier layer using the pre-existing embeddings from the frozen layers for a specific task. In our case, this task is to classify distracted driving actions from visual data. We evaluate the performance of the whole framework on a corresponding distracted driving dataset. As per the primary model [4], we implement five CLIP visual backbones- ViT-L/14, ViT-B/16, ViT-B/32, RN101 and assess each of their performance individually.

The Zero-shotCLIP, Single-frameCLIP and Multi-frameCLIP frameworks have input  $I \in \mathbb{R}^{3 \times H \times W}$  where

$I$ ,  $H$ , and  $W$  represent the input image, image height and image width, respectively. The Zero-shotCLIP makes predictions on raw frames without requiring any training. The key difference between the other two frameworks is that Single-frameCLIP makes predictions looking at a single frame and the Multi-frameCLIP makes predictions on a stack of frames conducting a majority vote at the classification layer. For both frame-based and video-based CLIP all the layers up to the classifier layer were kept frozen and we only finetuned the last trainable layer (shown in Fig. 2).

#### 2) Video-based model

The VideoCLIP model has a similar structure to the frame-based model shown in Fig. 2, but uses a different CLIP visual encoder and model input. It utilizes a branch called S3D (separable 3D CNN) [37], a video processing backbone based on 3D-CNN, which takes a video  $V \in \mathbb{R}^{S \times 3 \times H \times W}$  as input and encodes the video into a feature vector  $F$ . Here  $S$ ,  $V$ ,  $H$ , and  $W$  represent the number of frames, image height and image width, respectively. In our experiments, the number of frames  $S$  is set as 30, indicating that the VideoCLIP model uses 30 frames and synthesizes them into a short video clip. The rest of the training process is similar to the frame-based CLIP. In the training process, if the cosine similarity between the video feature and its corresponding text feature is high, the distance between their feature vectors is minimized. It should be highlighted that both the Multi-frameCLIP and VideoCLIP operate on successive frames, thereby capturing the temporal context of a given distracted action. A majority vote strategy is employed at the final stage by both frameworks. The key difference between these two models is illustrated in Fig. 1, with a comprehensive discussion provided in Section IV.

Fig. 3 shows the overall sampling procedure that we follow for our experiments. The blue block on the left shows some sample frames from the original video, which has a frame rate of 30 frames per second (FPS). The yellow blocks show the sampled frames at corresponding sampling rates. Due to the CLIP network’s limitations in processing numerous frames simultaneously, we sample the frames from the video data at various sampling rates and created a 30-frame-long video piece to feed into the VideoCLIP network. From Fig. 3, it could be observed that when the sampling rate is high, such as 20 FPS, the consecutive frames exhibit little semantic differences, and the video snippet (built from 30 frames) covers less time duration. In contrast, if the sampling rate is low, the video snippet could span longer time duration, with greater semantic differences between two consecutive frames. We perform a series of experiments to determine the best sampling rate for the video-based framework, discussed in Section IV, and the results of the experiments are explained in Section V.

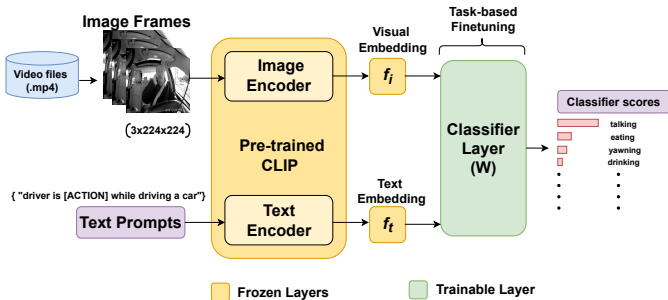


Fig. 2. The proposed multimodal Single-frameCLIP framework that exploits the pretrained CLIP architecture to extract vision-text semantic information.

## IV. EXPERIMENTS

### A. Dataset

We evaluate the proposed frameworks on two commonly used distracted driving datasets, namely SynDD1 [38] and StateFarm [39]. Both of these datasets serve as standard benchmarks for the analysis of distracted driving behavior, typically providing annotated images and videos that correspond to

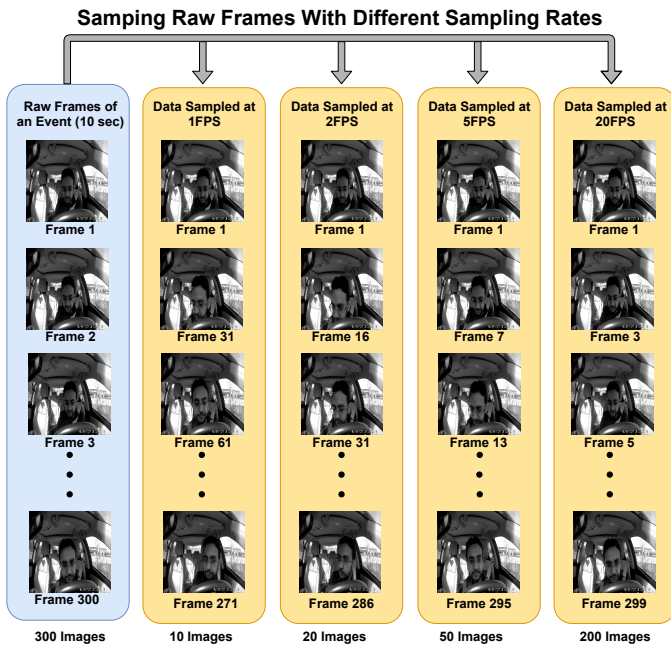


Fig. 3. The raw data is shown in the blue box, which contains 300 frames of an event lasting for 10 seconds. In other words, each second covers 30 frames. We sample frames with different sampling rates from the raw data, and the sampled data is shown in the yellow box. For example, when the sampling rate is 2 frames per second (FPS), we sample two images from 30 raw frames covered in each second. Since the raw data lasts for 10 seconds, we will have a total of 20 sampled images in the end.

diverse distracted driving behaviors exhibited by participants. Each dataset comes with an individual driver ID for each participant. The selection of these datasets was motivated by the availability of unique driver IDs for each participant, enabling us to conduct ‘leave a set of drivers out’ experiments, ensuring the absolute separation of testing and training sets. For our experiments, we utilize the driver IDs to separate out a specific set of drivers only for testing. In addition, we assess the performance of our distracted driving models through a  $k$ -fold cross-validation approach, executed on each driver set. Then we calculate the average accuracy across all  $k$  folds and report it as the final accuracy of the frameworks. Moreover, we analyze the proposed frameworks’ performances for each dataset separately and present the resulting analyses in detail in the subsequent sections.

**B. SynDD1 dataset**

The SynDD1 dataset [38] is a recent addition to distracted driving datasets, offering insights into naturalistic distracted driving behaviors. The dataset includes videos of distracted driving events, recorded by cabin cameras inside the vehicle. A total of 18 participants performed various in-car driving activities, which were recorded (as video) from three distinct camera angles - the dashboard camera, the rear-view mirror camera, and the right-side window camera. The videos have two types of annotation files - gaze activity and distracted activity. The first row of Fig. 4 shows some sample frames of distracted driving actions from the dashboard camera view. There are 18 driving activities performed by the participants

including ‘normal forward driving’, ‘drinking’, ‘phone call (right hand)’, ‘phone call (left hand)’, ‘eating’, ‘texting (right hand)’, ‘texting (left hand)’, ‘hair and makeup’, ‘reaching behind’, ‘adjusting control panel’, ‘pick up something from the floor (driver seat)’, ‘pick up something from the floor (passenger seat)’, ‘talking to the passenger at right’, ‘talking to the passenger at the backseat’, ‘yawning’, ‘hand on head’, ‘singing’, ‘shaking or dancing’. Each video file comes with annotations, including action types, the start and end time of an action, the appearance of the participant and so on. Therefore, we have the start and end time of a particular distracted action and their corresponding time duration. Each distracted driving video in the dataset has a frame rate of 30 FPS, with each frame possessing an RGB resolution of (1080,1920,3). For the purpose of this study, we consider the distracted behaviors of 14 drivers, thereby generating a more concise distracted driving dataset. For further generalization, we merge the similar action categories and consider eight distinct distracted actions shown in Table I. This modification allowed us to compare the results of our proposed frameworks for both datasets with an almost consistent number of classes. Fig. 5 shows the distribution of the distracted driving action duration (in seconds) across eight distinct distracted driving action classes derived from the SynDD1 dataset. The X-axis enumerates the eight specific distracted driving action categories, while the Y-axis represents the corresponding duration (sec) of these actions aggregated across all drivers. The average action duration across all categories is approximately 18.692 seconds. The median and spread of the action duration suggest an almost uniform distribution. Consequently, the probability of a specific distracted driving action being more prevalent than others within the examined range is nearly non-existent. The likelihood of occurrence for all durations of distracted driving actions is essentially equal. However, it is important to note that perfectly uniform distributions are rare to see in real-world scenarios, especially in studies related to human behavior.



Fig. 4. Sample dashboard camera frames from SynDD1 dataset- (a) drinking, (b) adjusting hair, (c) talking to phone (right hand); Statefarm dataset- (d) drinking, (e) adjusting hair, (f) talking to phone (left hand)

TABLE I  
DISTRACTED DRIVING ACTION CATEGORIES FOR SYNDD1 DATASET

ID	distracted driving prompt description
0	driver is adjusting his or her hair while driving a car
1	driver is drinking water from a bottle while driving a car
2	driver is eating while driving a car
3	driver is picking something from floor while driving a car
4	driver is reaching behind to the backseat while driving a car
5	driver is singing a song with music and smiling while driving
6	driver is talking to the phone on hand while driving a car
7	driver is yawning while driving a car

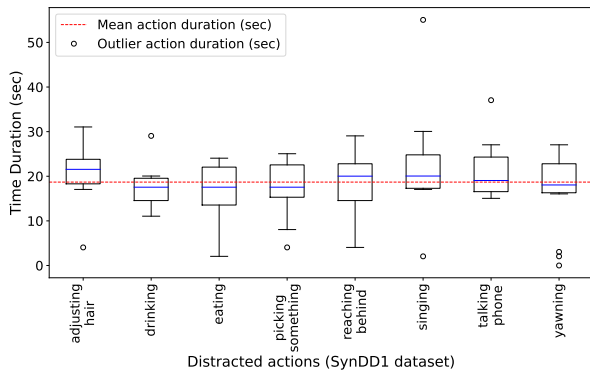


Fig. 5. The distribution of the time duration (sec) across eight distracted driving actions from the SynDD1 dataset. The mean action duration is 18.692 seconds. The median and spread of the action duration suggest an almost uniform distribution, demonstrating a balance in the action categories we use.

### C. StateFarm Dataset

The StateFarm dataset [39] serves as another benchmark dataset for distracted driving behavior analysis, providing only image (RGB) data. The images were captured from an in-cabin camera positioned on the right-side window, offering a right-side perspective of the driver, as seen in the second row of Fig. 4. Data was collected from 26 participants, and the total number of image frames is 22,424. Similar to the SynDD1 dataset, the StateFarm dataset includes unique driver IDs for each participant, which enables us to perform driver-level k-fold cross-validation. However, it does not provide information on the action duration, start, or end times of actions as the labels pertain only to image frames. There are ten distracted driving activity categories in total- ‘normal driving’, ‘texting (right hand)’, ‘talking on the phone (right hand)’, ‘texting (left hand)’, ‘talking on the phone (left hand)’, ‘operating the radio’, ‘drinking’, ‘reaching behind’, ‘hair and makeup’, ‘talking to a passenger’. The images have a resolution of (640,480,3). We consider all the drivers and ten action categories for our experimental analysis.

### D. Experiment Setup - ZeroshotCLIP and Single-frameCLIP

Our overall approach is depicted in Fig. 2. First, we explore the zero-shot transfer capability of the CLIP model on distracted driving data in the Zero-shotCLIP framework. Then, we explore the task-based finetuning route to evaluate the “task learning capability” of our proposed Single-frameCLIP framework. For the Zero-shotCLIP experiment, there is no training associated, and we simply predict the class-level confidence score of the pre-trained CLIP model on raw

image frames (224x224x3). Next, we assess the representation learning capability of the pre-trained CLIP model on the distracted driving dataset in the Single-frameCLIP framework. We add an extra linear classifier layer on top of the pre-trained CLIP model architecture and train the single layer on distracted driving datasets (SynDD1, StateFarm). For training the linear classifier (see CLIP [4]), we use image frames of input size (224x224x3) collected from the above two datasets. We utilize a batch size of 100 and a learning rate of 0.001. While training the Single-frameCLIP, we kept the pre-trained layers frozen and updated only the final layer based on the cross-entropy loss. Fig. 1 provides a visual representation of this approach, which generates predictions on a frame-by-frame basis. To illustrate this process, let’s consider a 10-second event sampled at a rate of 30 frames per second with a total of 300 frames (depicted in Fig. 1 by the yellow box). For each of these frames, the Single-frameCLIP model generates a prediction, beginning with the first frame (Image-1), and subsequently for each following frame (Image-2, Image-3, etc). In addition, we perform 7-fold and 8-fold cross-validation based on the driver ID for the SynDD1 and StateFarm datasets, and report the average accuracy in Section V. Moreover, we experiment with various CLIP backbones (see CLIP [4]) and other hyperparameters. Notably, the original CLIP model employs semantic information in text labels rather than the traditional one-hot labels, which require providing a textual description or prompt for each action category. Therefore, we utilized a full sentence as a prompt for describing the image frame of each action class instead of a single word. The prompt descriptions for the SynDD1 dataset are shown in Table I. As reported in [4], we consider manually fine-tuning and rephrasing the prompt sentences for our experiments, an area that can be further optimized in future work.

### E. Experiment Setup - Multi-frameCLIP

The Multi-frameCLIP framework is specifically designed to analyze sequences of consecutive frames from distracted driving videos. This approach extends upon the Single-frameCLIP, concluding with an additional majority voting step applied across consecutive frames to generate the final event prediction. The majority voting method allows our framework to make a single prediction on a particular action event. During the first step of training, this framework is provided with the frames between the start and end times of a specific action within the video footage. Following this, the Single-frameCLIP model is applied to each frame falling within these timestamps, providing individual predictions for each frame. A majority voting method is then employed to produce a final prediction. If this prediction aligns with the ground truth action label for that segment of the video, it is considered a correct prediction. This entire process is visually represented in Fig. 1. From the raw video data, we sample frames at varying rates (as depicted in Fig. 3). Let’s consider a 10-second event, containing 300 frames captured at a rate of 30 FPS (shown by the yellow box). The Single-frameCLIP model is employed to make predictions for each of these frames, starting with the first frame (Image-1), and then sequentially

progressing (Image-2, Image-3, and so on). Finally, a majority vote among all the individual frame predictions is taken to make a final prediction for the entire 10-second event in the video. This method allows Multi-frameCLIP to extend Single-frameCLIP’s capability by incorporating a temporal understanding of the events in a video. To ensure robust results, we conducted cross-validation experiments with sampling rates of 1, 2, 5, 20, and 0.5 frames per second.

#### F. Experiment Setup - VideoCLIP

This framework, referred to as VideoCLIP, is an adaptation of the frame-based CLIP model. It incorporates a 3D Convolutional Neural Network (CNN) backbone, specifically designed for video processing. For additional information, readers can refer to [40]. The key difference in this model is its consideration of the temporal information of video data when making a prediction. When the model needs to make a prediction about a particular frame, it does not just look at that single frame. Instead, it combines 14 frames that come before and 15 frames that come after the target frame to form a small clip. A total of 30 frames are used together for prediction. This video piece is fed into the pre-trained CLIP backbone and finally, majority voting is conducted to produce the final prediction. Fig. 1 shows an overview of the VideoCLIP model pipeline. This technique enables the model to consider not only the content of the targeted frame but also the preceding and subsequent frames. In this way, the network can perform classification with more complete temporal information. In this experiment, the learning rate and batch size are set as 0.0003 and 5, respectively, and Adam [41] optimizer is used. Similar to above, we split the drivers into two non-overlapping sets (training and testing) to evaluate the performance on never-before-seen drivers. Finally, we perform seven-fold cross-validation on the data with sampling rates of 1,2,5 and 20 frames per second.

#### G. Experiment Setup for CLIP vs. Other Models

For performance comparison, we further trained several mainstream CNN backbones, which are commonly used for distracted driving recognition. We considered five different backbones, namely AlexNet [42], VGG16 [16], MobileNetv2 [43], ResNet18 and ResNet50 [25], and used them on frames sampled from videos in SynDD1 dataset. We used ImageNet pre-trained weights and fine-tuned the models with a learning rate of 0.001 and a batch size of 64. We used Adam [41] as the optimizer. We report the experimental results and outcome of our observation in Section V.

## V. RESULTS

### A. Performance of CLIP-based Frameworks

We present the performance of various CLIP-based frameworks on two distracted driving datasets in Table II. On the SynDD1 dataset, VideoCLIP with an optimal hyperparameter setting demonstrated superior performance with a Top-1 accuracy of 81.85% and a Top-3 accuracy of 91.96% for

distracted driving recognition. This was followed by the Multi-frameCLIP framework with an optimal hyperparameter setting. Single-frameCLIP and Zero-shotCLIP reported lower Top-1 accuracies on the SynDD1 dataset compared to the Statefarm dataset.

TABLE II  
PERFORMANCE OF CLIP-BASED  
FRAMEWORKS ON DISTRACTED DRIVING DATASETS

Framework	SynDD1		StateFarm	
	Top-1	Top-3	Top-1	Top-3
Zero-shotCLIP	54.00	74.50	58.22	67.63
Single-frameCLIP	57.35	82.25	<b>83.15</b>	<b>95.75</b>
Multi-frameCLIP	70.36	75.38	-	-
VideoCLIP	<b>81.85</b>	<b>91.96</b>	-	-

On the StateFarm dataset, only Single-frameCLIP and Zero-shotCLIP were evaluated due to the absence of video data, which is a prerequisite for Multi-frameCLIP and VideoCLIP. Single-frameCLIP outperformed Zero-shotCLIP with optimal hyperparameter setting, achieving a Top-1 accuracy of 83.15% and a Top-3 accuracy of 95.75%.

These results highlight the effectiveness of VideoCLIP and Multi-frameCLIP in leveraging temporal information from video data for improved performance. It is important to note that we conduct comprehensive testing across various hyperparameter settings and select the parameters that deliver the highest performance for our proposed models. We refer to this setting as the “optimal hyperparameter setting”. A detailed analysis of these results and a discussion of the optimal hyperparameter setting are presented in the following sections.

#### 1) Zero-shotCLIP results

For the zero-shot experiments, we test the Zero-shotCLIP model on the distracted driving dataset without any prior training. The model encounters previously unseen frames extracted from distracted driving datasets. The RGB input images are resized to a resolution of 224x224x3. During the zero-shot evaluation, the framework extracts visual and textual features from the input images and corresponding textual prompts, respectively. Subsequently, the cosine similarity between these visual and textual features is computed, resulting in a ranked list of the most probable classes based on their similarity scores. The zero-shot transfer result for eight classes on the SynDD1 dataset is presented in Table III for different CLIP backbones. It can be seen that the ViT-L/14@336px vision transformer-based Zero-shotCLIP outperforms other variants in terms of Top-1 accuracy. It should be noted that the ViT-L/14@336px backbone processes input images at a higher RGB resolution (336x336x3). The key observation from these results is that Zero-shotCLIP demonstrates 74.5% Top-3 accuracy in recognizing distracted driving without requiring dataset-specific training.

#### 2) Single-frameCLIP results

We present the performance of the Single-frameCLIP model with optimal hyperparameter setting on the StateFarm and SynDD1 datasets in Table IV. Single-frameCLIP results showcase the advantage of task-based fine-tuning. For the StateFarm dataset, the Single-frameCLIP model with the CLIP-

TABLE III  
ZERO-SHOT TRANSFER ON SYNDD1 DATASET

CLIP visual backbone	Top-1 accuracy	Top-3 accuracy
ViT-L/14	53.50	<b>74.50</b>
ViTL/14@336px	<b>54.00</b>	65.00
ViT-B/16	47.50	64.50
ViT-B/32	38.00	45.50

L/14 backbone achieved a Top-1 accuracy of 81.85%. On the SynDD1 dataset, the same model reached a Top-1 accuracy of 57.35%. The results further confirm the robustness and effectiveness of the CLIP-L/14 backbone in the Single-frameCLIP model for the task of distracted driving action recognition. It should be noted that the task’s complexity and the specifics of the datasets may account for the difference in accuracy scores between the two datasets.

TABLE IV  
SINGLE-FRAMECLIP RESULTS WITH OPTIMAL HYPERPARAMETERS

Single-frameCLIP backbone	Dataset	Camera-view	Top-1 accuracy
CLIP-L/14	StateFarm	Dashboard	83.15
CLIP-L/14	SynDD1	Dashboard	57.35

### 3) Multi-frameCLIP results

Our Multi-frameCLIP framework involves employing majority voting over a set of frames to determine the final prediction of an action class in a video. We investigate various sampling rates of 0.5, 1, 2, 5, and 20 frames per second, subject-level cross-validation along with different camera views and CLIP backbones. The result with the optimal setting is presented in Table V. The best performance on the SynDD1 dataset is achieved with the CLIP-L/14 backbone from the dashboard camera-view footage sampled at 1 frame per second. This setting provided a Top-1 accuracy of 70.36%. We have observed that the model achieves the peak performance at a sampling rate of 1 FPS. Any increase in the sampling rate resulted in a decline in accuracy (as shown in Table X), since the inclusion of similar-looking frames acts as a form of noisy signal in the majority voting pool. On the other hand, reducing the sampling rate below 1 compromised performance, since critical temporal information that is essential for final action prediction gets overlooked. Therefore, we can conclude that 1 FPS is the optimal sampling rate for the Multi-frameCLIP model to adequately capture relevant temporal information. The main advantage of this model is that it processes several frames simultaneously, exploiting the temporal information between consecutive frames. This approach, combined with the high-level semantic understanding of the CLIP model, resulted in an improved performance, as evidenced by the Top-1 accuracy. The optimal hyperparameters were determined through a series of experiments to optimize the model’s overall performance.

### 4) VideoCLIP results

Similar to Multi-frameCLIP, we conducted a series of tests to obtain the optimal hyperparameter setting for the VideoCLIP model and report the results obtained on the SynDD1

TABLE V  
MULTI-FRAMECLIP RESULTS WITH OPTIMAL HYPERPARAMETERS

Multi-frameCLIP backbone	Dataset	FPS	Camera-view	Top-1 accuracy
CLIP-L/14	SynDD1	1	Dashboard	70.36

dataset in Table VI. The best performance of 81.85% Top-1 accuracy is achieved with the VideoCLIP built on the CLIP-L/14 backbone and with a sampling rate of 20 frames per second. The performance achieved by the VideoCLIP model validates its efficacy in understanding distracted actions from driving video footage. We have observed that the sampling rate has a significant effect on the final accuracy. Moreover, in contrast to Multi-frameCLIP, VideoCLIP uses a sliding window of 30 frames, and employs a majority voting scheme on the outputs of these small video clips. In our experiments, the VideoCLIP network achieved the best performance when the sampling rate was 20 FPS. If the sampling rate is too small, e.g. 1 FPS, there will be one frame sampled from every second of an activity. Since VideoCLIP uses 30 frames to build a clip, this clip will span 30 seconds which can be longer than the action and confuse the network. For example, an action video lasting 20 seconds should contain 20 frames, however, in these 20 frames, only 10 frames contain the valid information of that action for prediction. If we sampled 30 frames from those 20 frames to make up a window as the input to the network, most frames in the window are noise. In addition, the sliding window approach in VideoCLIP provides a more holistic representation of the video data, which leads to improved prediction accuracy. In the following sections, we will delve into the performance of our models under real-world variabilities and scrutinize the model’s efficacy across diverse scenarios.

TABLE VI  
VIDEOCLIP RESULTS WITH OPTIMAL HYPERPARAMETERS

VideoCLIP backbone	Dataset	FPS	Camera-view	Top-1 accuracy
CLIP-L/14	SynDD1	20	Dashboard	81.85

## B. Performance Comparison with Other Works

In this section, we present a performance comparison of our proposed CLIP-based frameworks (both frame-based and video-based) with traditional distracted driving recognition models.

### 1) Single-frameCLIP vs. Traditional Models

In this section, we compare the performance of the Single-frameCLIP model with traditional distracted driving backbones, namely ResNet18, Mobilenetv2, and AlexNet, on both StateFarm and SynDD1 datasets. The Top-1 accuracy values are presented in Tables VII, VIII and Fig. 6. It should be noted that, across all model comparisons in our experiments, we maintain consistency by using the dashboard camera view (which yielded the best results) along with the same action classes. The detailed experiment results for ten distracted

driving action classes on the StateFarm dataset are shown in Table VII, where the first column entries represent the drivers used in the testing split. This data split involved leaving three drivers out for testing. For instance, p002p014p012 signifies that drivers with IDs p002, p014, and p012 were set aside for the first fold. The remaining drivers were used for the training set. We follow this procedure eight times, each time keeping different groups of drivers separate for testing. We conduct 8-fold driver-level cross-validation on the StateFarm dataset. The other columns display the Top-1 accuracy of each model for different test splits. The last row provides an average Top-1 accuracy for each model across all folds. Amongst all the models, the Single-frameCLIP model with ViT-L/14 architecture emerged as the best performing, achieving an average Top-1 accuracy of 83.15%. Fig. 6 visually represents these results. The bars illustrate the average Top-1 accuracy of the models, while the vertical lines on the top indicate the variance in Top-1 accuracies across all eight folds.

TABLE VII  
SINGLE-FRAMECLIP VS. TRADITIONAL MODELS:  
TOP-1 ACCURACY ON STATEFARM DATASET

Test Drivers	ResNet18	Mobilenetv2	AlexNet	CLIP-L/14
p002p014p012	72.81	74.09	68.23	75.66
p015p016p021	81.35	82.16	75.33	88.12
p024p022p026	87.11	86.16	81.67	89.03
p041p039p035	87.17	85.60	87.12	90.27
p042p045p047	84.00	81.91	81.72	89.03
p051p049p050	88.72	81.48	70.38	78.13
p061p056p052	86.17	82.50	75.16	72.39
p066p072p064	74.14	66.45	59.14	71.46
Average accuracy	82.68	80.04	74.84	<b>83.15</b>

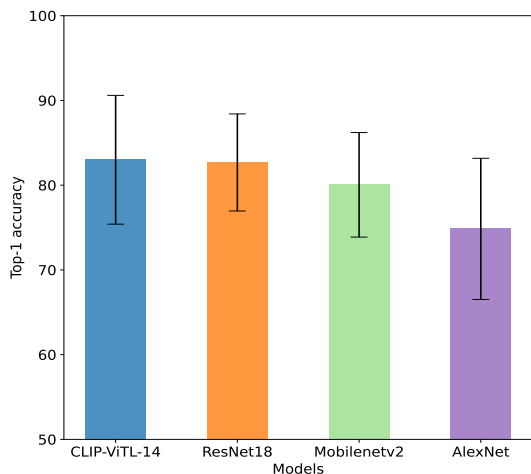


Fig. 6. The average Top-1 accuracy of Single-frameCLIP and other baselines on the StateFarm dataset. We perform 8-fold cross-validation and show the mean and variance of Top-1 accuracy values across all the folds along the Y-axis.

The comparison results obtained with the eight distracted driving classes in the SynDD1 dataset are presented in Table VIII. Similar to the experiments on the StateFarm dataset, this experiment involved 7-fold driver-level cross-validation leaving two drivers out for testing in each fold.

The third column in Table VIII represents the average Top-1 accuracy across all the 7-folds. The results reveal that the CLIP-L/14 model outperformed others, achieving a Top-1 accuracy of 57.347% (average accuracy across 7-folds). The remaining models followed with lower accuracies, with CLIP-B/16 achieving 48.940%, and CLIP-RN101 at 48.521%. In conclusion, the Single-frameCLIP model with the ViT-L/14 architecture demonstrated superior performance in terms of Top-1 accuracy both in the StateFarm and SynDD1 datasets. In contrast, traditional models fell short in achieving performance close to that of the CLIP-L/14 model.

TABLE VIII  
SINGLE-FRAMECLIP-BACKBONES VS. TRADITIONAL MODELS:  
TOP-1 ACCURACY ON SYNDD1 DATASET

Models	Backbones	Average Top-1 accuracy
Single-frameCLIP	CLIP-L/14	<b>57.347</b>
	CLIP-B/16	48.940
	CLIP-RN101	48.521
	CLIP-B/32	35.382
Traditional Models	ResNet18	42.621
	Mobilenetv2	36.102
	AlexNet	13.712

## 2) Dataset size vs. Performance

In an effort to analyze the performance of the Single-frameCLIP model with smaller amounts of training data, a series of experiments were conducted utilizing a progressively reduced training dataset. In this experiment, we train the traditional models and our proposed CLIP-based frameworks in a similar experimental setting. From the StateFarm dataset, we separate 3 drivers (drivers with ID p012, p014, p021) for testing and progressively removed 4 drivers from the training set to create a smaller training set, which is 80%, 60%, 40%, and 20% of the original training set. For this process, instead of randomly removing frames, we reduce the training data based on the driver ID, since in real-world scenarios the model will be expected to generalize its learning to new, unseen drivers. The percentage of training data, the number of drivers present in those splits, and the number of samples are shown in Table IX. For this experiment on the StateFarm dataset, we employ an 8-fold cross-validation scheme where we excluded three drivers (driver ID p012, p014, p021) from every fold and used them as test subjects. We picked CLIP-ViT/L-14 backbone for the Single-frameCLIP. All the models used the same training samples and were finally tested on the same test set. The performances are presented in Fig. 7. The results suggest that reducing the size of the training set does not necessarily compromise the Single-frameCLIP model's performance. Unlike the other models assessed, which displayed a decrease in accuracy, the Single-frameCLIP model maintained its performance levels consistently even when the quantity of training data was reduced to 20% of the original amount.

## 3) Multi-frameCLIP vs. Traditional Models

We present the Top-1 accuracy results of Multi-frameCLIP and traditional models on the SynDD1 dataset in Table X. The evaluated models include several versions of CLIP backbones,

TABLE IX  
TRAINING DATASIZE FOR REDUCED TRAINING SET

Percentage of training data	No. of drivers in training	No. of samples in training	Test set driver IDs
80%	18	16163	p012p014p021
60%	14	12900	p012p014p021
40%	9	8949	p012p014p021
20%	5	5649	p012p014p021

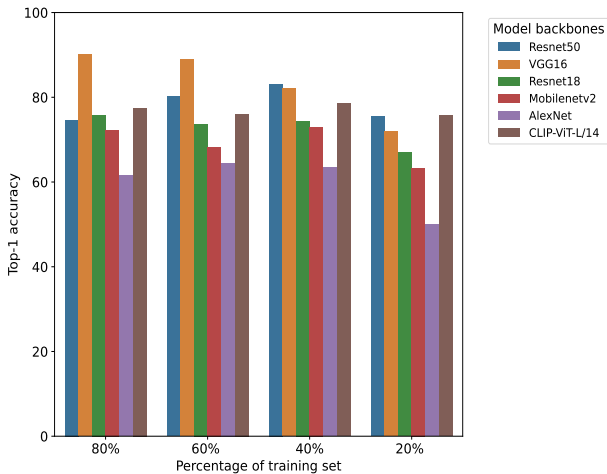


Fig. 7. Performance comparison of the Single-frameCLIP model and traditional models trained on varying proportions of the StateFarm dataset. Training sets of 80%, 60%, 40%, and 20% were created by progressively removing drivers based on their ID. The figure reports the models’ average accuracies obtained through an 8-fold cross-validation scheme based on driver ID.

ResNet18, ResNet50, Modilenetv2, AlexNet, and Vgg16. The results are presented for different sampling rates and dashboard camera view as this view yielded the best results. From the table, we can see that the highest Top-1 accuracy of 70.36% is achieved by CLIP-L/14 with a sampling rate of 1 FPS. On the lower end, AlexNet and Vgg16 appear to perform the worst across all sampling rates, with accuracy rates hovering around 12.62%. In general, the accuracy appears to vary depending on the model and the sampling rate (discussed in the following sections), indicating that these are significant factors in performance on the SynDD1 dataset.

### C. Hyperparameters and Ablation Studies

In this section, we discuss how various real-world parameter settings, such as the sampling rate, camera location and presence of different distracted driving classes can impact the performance of our proposed CLIP-based frameworks.

### 1) Sampling Rate

We present the performance of the Multi-frameCLIP model tested at various sampling rates on the SynDD1 dataset in Table X. We perform a 7-fold cross-validation experiment with different sampling rates on the Multi-frameCLIP model and other commonly used distracted driving backbones to see the effect of sampling rates on model performance. The results indicate that the CLIP-L/14-based Multi-frameCLIP achieves the highest top-1 accuracy at 1 FPS sampling rate, with an accuracy of 70.36%. This was the highest accuracy achieved across all tested models and sampling rate settings for this experiment. In comparison, the lowest accuracy values were consistently provided by AlexNet and Vgg16 models across all FPS settings, with both models achieving an accuracy of 12.62%. The results also suggest that varying the sampling rate can impact the performance of the models. For example, the performance of the CLIP-L/14 model decreased from 70.36% accuracy at 1 FPS to 62.08% at 5 FPS and to 61.25% at 20 FPS. These findings suggest that the optimal sampling rate may vary depending on the specific model employed. The changes from one frame to the next are more significant at a 1 FPS sampling rate, which helped the model make more accurate predictions. Therefore, 1 FPS is the optimal sampling rate for the Multi-frameCLIP model under the conditions of our study.

Table XI shows the performance of the VideoCLIP model on the SynDD1 dataset at different sampling rates of 1 FPS, 2 FPS, 5 FPS, and 20 FPS. We perform seven-fold cross-validation on the VideoCLIP model to see the effect of sampling rates on model performance. The ‘Mean’ column reports the average accuracy across all folds for each respective FPS setting. The results indicate that VideoCLIP achieves the highest Top-1 accuracy at 20 FPS, with an accuracy of 81.85%. A higher FPS results in a better temporal resolution, allowing the model to capture more subtle changes and movements that occur between frames. Consequently, the model may be better equipped to understand and predict based on these small changes. However, the exact impact of sampling rate would depend on the specific characteristics of the dataset and the downstream task.

### 2) Class-level analysis

We illustrate the class-level precision, recall, and F1-scores of Single-frameCLIP on the SynDD1 dataset in Table XII. In this table, we analyze all eight classes to understand the most challenging actions to classify. In addition, we demonstrate the confusion matrix of the action classes in Fig. 8. We have found that classes such as “eating,” “singing and smiling,” and “yawning” exhibited lower performance metrics,

TABLE X  
MULTI-FRAMECLIP AT DIFFERENT SAMPLING RATES ON SYNDD1 DATASET

Sampling Rate	CLIP-L/14	CLIP-B/16	CLIP-RN101	CLIP-B/32	ResNet18	ResNet50	Modilenetv2	AlexNet	Vgg16
0.5FPS	56.67%	52.98%	48.57%	39.52%	43.51%	39.52%	41.31%	12.62%	12.62%
1FPS	<b>70.36%</b>	60.01%	55.60%	41.65%	47.55%	43.49%	33.65%	12.56%	12.56%
2FPS	59.46%	53.04%	50.36%	37.68%	40.59%	38.75%	34.11%	12.62%	12.62%
5FPS	62.08%	59.34%	49.34%	36.96%	43.21%	39.70%	48.75%	12.62%	12.62%
20FPS	61.25%	61.13%	49.35%	36.96%	46.79%	40.71%	45.12%	12.62%	12.62%

TABLE XI  
VIDEOCLIP AT DIFFERENT SAMPLING RATES ON SYNDD1 DATASET

Sampling Rate	Fold0	Fold1	Fold2	Fold3	Fold4	Fold5	Fold6	Mean
1FPS	<b>93.75%</b>	87.50%	87.50%	75.00%	60.00%	50.00%	68.75%	74.64%
2FPS	81.25%	87.50%	87.50%	87.50%	66.67%	68.75%	75.00%	79.17%
5FPS	87.50%	81.25%	<b>93.75%</b>	75.00%	66.67%	56.25%	68.75%	75.60%
20FPS	87.50%	<b>93.75%</b>	87.50%	<b>93.75%</b>	<b>66.67%</b>	<b>68.75%</b>	<b>75.00%</b>	<b>81.85%</b>

indicating that these categories pose greater challenges for the framework to classify correctly. These action classes appeared to generate similar image features, leading to a higher rate of misclassification. To further illustrate this, Fig. 9 provides visual examples of instances where the Single-frameCLIP model incorrectly classified actions, comparing the model’s outputs against the ground truth.

TABLE XII  
SINGLE-FRAMECLIP: PRECISION, RECALL, AND F1-SCORE ON SYNDD1

Action classes	Precision	Recall	F1-score
adjusting hair	0.51	0.74	0.60
drinking water	0.70	0.86	0.78
eating	0.60	0.31	0.41
picking up something	0.76	0.96	0.85
reaching behind	0.79	0.94	0.86
singing and smiling	0.44	0.30	0.36
talking to the phone	1.00	0.77	0.87
yawning	0.56	0.42	0.48

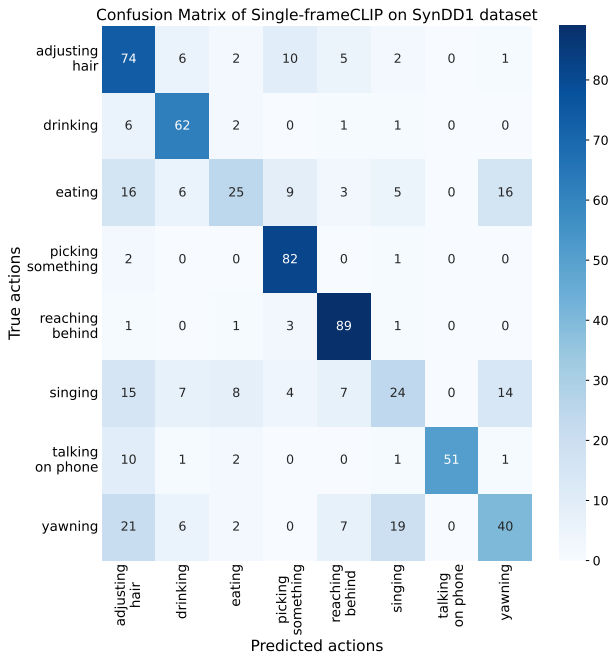


Fig. 8. Confusion matrix (normalized) of Single-frameCLIP model on SynDD1 dataset. It shows the classes - “eating”, “yawning” and “singing” - for which Single-frameCLIP struggles to classify the distracted driving action.

### 3) Merging vs. Removing Classes

To fully understand the impact of the challenging classes on overall model performance, we pursue two additional experiments: merging and removing classes. Our initial focus

was to explore how the overall model performance is influenced by either merging or removing classes that are more challenging to predict accurately. From the previous analysis, we identify that the Single-frameCLIP model has difficulty in accurately predicting the “singing”, “eating” and “yawning” classes compared to others. Table XIII reflects our findings, which are categorized into three different experimental settings. The first row shows the outcome following the removal of the three challenging classes with three camera views. This modification resulted in an average F1 score of 0.763 and a mean accuracy of 75.62%. The second row illustrates the outcome of merging the three challenging classes with three camera views. This scenario led to a mean F1 score of 0.698 and an average accuracy of 69.41%. The third row provides the results obtained from an experiment in which the three challenging classes were removed and only the dashboard camera view was considered. This experimental setup led to an average F1 score of 0.873 and a mean accuracy of 87.08%. In conclusion, the optimization of the camera views, combined with the adjustment of the challenging classes, resulted in a significant improvement in the model’s performance.

### 4) Effect of Camera Views

In this section, we investigate the effect of camera position on our framework’s performance. In Table XIV, we present the Single-frameCLIP accuracy for five distracted classes, considering three distinct camera views. The outcomes of these experiments suggest that the use of a single camera view, particularly the dashboard view, yields superior results when compared to other camera views on the SynDD1 dataset. These results underscore the importance of camera perspective in driver distraction detection tasks. The dashboard camera view appears to provide the most effective angle for capturing driver behaviors due to the direct line of sight and better visibility of driver action.

### D. Anecdotal Observation

In this section, we discuss the cases where our proposed frameworks struggle to perform well and investigate the possible reasons .

#### 1) Failure cases

We report some of the miss-classified frames by the Single-frameCLIP model on the SynDD1 dataset in Fig. 9 and the class-level confusion matrix in Fig 8. Analyzing the confusion matrix and the miss-classified frames, we conclude that the most challenging frames reside in the overlap of the three classes -“eating”, “yawning” and “singing” in the SynDD1 dataset. In addition, we manually look into the video files of the misclassified actions and noticed that these three classes are mostly dependent on specific hand or facial gestures.

TABLE XIII  
SINGLE-FRAME CLIP: REMOVING VS. MERGING CLASSES RESULTS ON SYNDD1 DATASET

Experiment type	No.of class	No.of camera-view	adjusting hair	drinking water	picking something	reaching behind	talking phone	sing+eat +yawn	Mean F1	Mean accuracy
Removing	5	3	0.64	0.71	0.84	0.82	0.80	-	0.763	75.62%
Merging	6	3	0.51	0.50	0.82	0.75	0.88	0.73	0.698	69.41%
Removing with dashboard-view	5	1	0.77	0.87	0.89	0.94	0.89	-	0.873	87.08%

TABLE XIV  
SINGLE-FRAMECLIP: EFFECT OF CAMERA-VIEW ON SYNDD1 DATASET

No. of class	Camera-view	Top-1 accuracy
5	Dashboard camera view	<b>87.640</b>
5	Rear mirror camera view	85.811
5	Right window camera view	76.056

Most of the time, it is quite complicated to decipher these activities from each other by looking at only a single frame. To address this complexity, the Multi-frameCLIP and VideoCLIP frameworks with a majority voting scheme were developed, wherein a stack of frames is assessed for a more accurate prediction score. This consideration contributed to the noted performance enhancement relative to the Single-frameCLIP model.

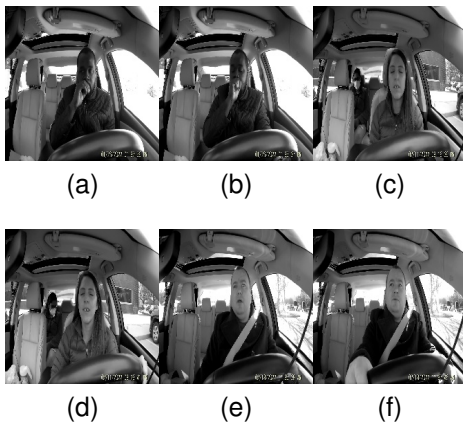


Fig. 9. Some example frames that were misclassified by the frameCLIP on SynDD1 dataset- (a) predicted: yawning, ground-truth: eating (b) actual yawning, (c) predicted: yawning, ground-truth: singing (d) actual yawning, (e) predicted: singing,ground-truth: yawning (f) actual singing

## 2) Frame-by-frame Analysis for Video Input

Fig. 10 presents the frame-by-frame analysis of video input for driver ID 25470 from the SynDD1 dataset using the Multi-frameCLIP and VideoCLIP models. The depicted plot conveys the dynamic probabilities of predictions produced by the Multi-frameCLIP and VideoCLIP models over the entire span of action. The vertical axis shows the moving average of the computed probabilities in relation to the individual frame numbers, represented by the horizontal axis. We observe distinct fluctuations between high and low probability scores, aligning with frames where the model either successfully or unsuccessfully classified the given action. Our analysis focused on two distinct actions - adjusting hair and singing,

at a sampling rate of 20 FPS. The representation of lower and higher probability scores from both models is clearly distinguished in this visualization. An important observation is the superiority of VideoCLIP’s prediction score over the entire course of action, compared to that of the Multi-frameCLIP model. Additionally, we notice that VideoCLIP demonstrates a stable and consistent performance, capturing low-probability frames and maintaining a consistent score throughout the video. In contrast, the Multi-frameCLIP model appears to struggle at certain frames. Therefore, we conclude that VideoCLIP has the capability to efficiently capture temporal information from videos significantly improving prediction accuracy while maintaining consistency. Moreover, the plot illustrates the superiority of both Multi-frameCLIP and VideoCLIP in extracting the temporal correlations among frames, thus providing insights into continuous actions that are challenging to get from isolated frames, as in the Single-frameCLIP scenario.

## VI. CONCLUSION

In this paper, we have introduced a vision-language modeling framework aimed at categorizing distracted driving behaviors from naturalistic driving data. Performance of various CLIP-based frameworks have been evaluated on two distracted driving datasets, namely SynDD1 and StateFarm. Compared to the Zero-shotCLIP model, the Single-frameCLIP model benefited from task-based fine-tuning with significant improvement in accuracy while failing to capture the temporal dynamics of a video. Further experiments have shown that Multi-frameCLIP and VideoCLIP can leverage temporal information from video data, which allows for a better understanding of actions, events and sequences within a video. VideoCLIP and Multi-frameCLIP frameworks have outperformed Single-frameCLIP by a significant margin. Overall, our proposed frameworks exhibit state-of-the-art performance at distracted action classification, as tested on two public datasets, and outperform traditional and widely used models. Our findings have also shown that, unlike the other models assessed, which displayed a decrease in accuracy, the Single-frameCLIP model could maintain its performance levels consistently even when the quantity of training data was reduced to 20% of the original amount. This study has also evaluated the efficacy of different CLIP-model variants, highlighting that their performance can be influenced by a variety of factors including variable training dataset size, sampling rates, and camera perspectives. These observations can contribute to the development of more robust driver assistance systems to understand driver distractions. This study emphasizes the real-world applicability and gen-

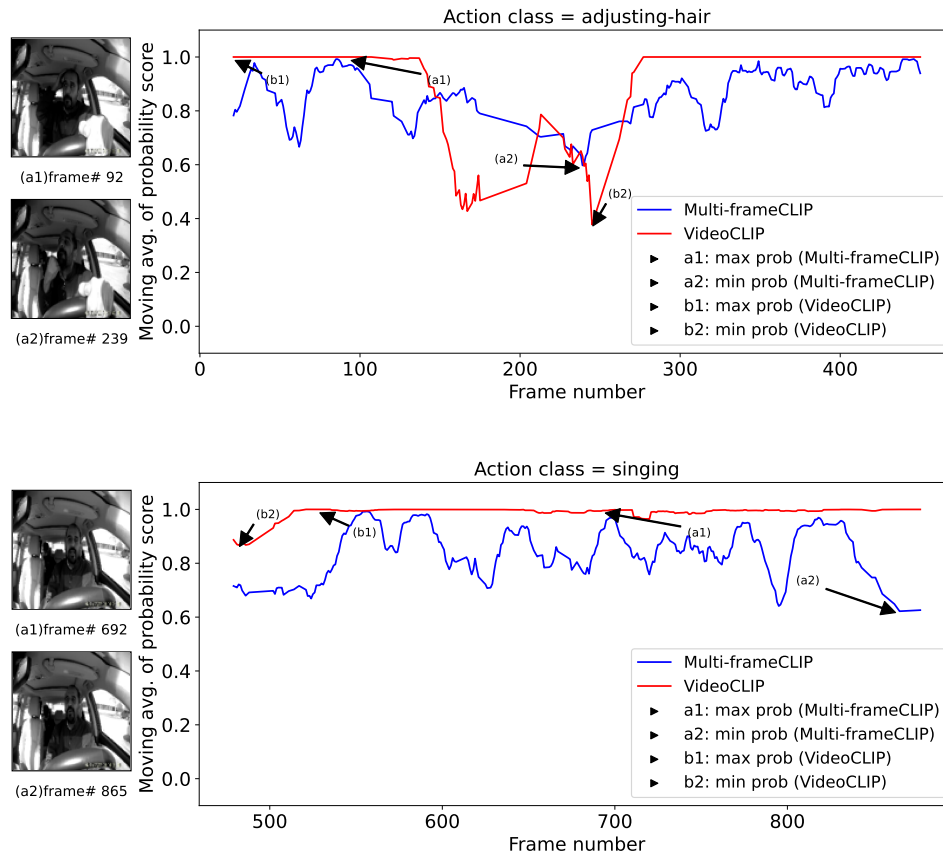


Fig. 10. This plot shows the predicted probability score vs. frame number. We analyze the Multi-frameCLIP and VideoCLIP model’s prediction probability scores for the entire action. We notice distinct changes in frames for high and low probability scores. This figure demonstrates that the VideoCLIP outperforms Multi-frameCLIP’s prediction scores offering a better approach to capturing temporal features. Therefore, VideoCLIP performs better in classifying actions on video data

eralizability of these models, while also pointing out areas for improvement, such as managing difficult classification categories and fine-tuning hyperparameters. Several future works could extend and refine our current CLIP-based driver distraction identification model. First, exploring the optimization of prompts for Vision-Language foundation models may enable the framework to extract more nuanced visual-textual relationships, leading to an improved classification. Second, the fusion of different camera views can be investigated as a means of providing a more comprehensive picture of driver behavior, potentially contributing to more accurate decision-making.

Moreover, the generalizability of our model across various scenarios and datasets presents another intriguing prospect. For instance, assessing whether the model could be fine-tuned on one dataset and subsequently deployed on another could further illustrate its versatility and effectiveness. Finally, systematic evaluations under diverse environmental conditions, such as varying lighting situations and data quality, could offer valuable insights into the model’s robustness and ability to function optimally under real-world driving circumstances.

## REFERENCES

[1] T. A. Dingus, F. Guo, S. Lee, J. F. Antin, M. Perez, M. Buchanan-King, and J. Hankey, “Driver crash risk factors and prevalence evaluation

using naturalistic driving data,” *Proceedings of the National Academy of Sciences*, vol. 113, no. 10, pp. 2636–2641, 2016.

[2] N. Moslemi, R. Azmi, and M. Soryani, “Driver distraction recognition using 3d convolutional neural networks,” in *2019 4th International Conference on Pattern Recognition and Image Analysis (IPRIA)*, 2019, pp. 145–151.

[3] S. Xie, C. Sun, J. Huang, Z. Tu, and K. Murphy, “Rethinking spatiotemporal feature learning: Speed-accuracy trade-offs in video classification,” in *Proceedings of the European conference on computer vision (ECCV)*, 2018, pp. 305–321.

[4] A. Radford, J. W. Kim, C. Hallacy, A. Ramesh, G. Goh, S. Agarwal, G. Sastry, A. Askell, P. Mishkin, J. Clark *et al.*, “Learning transferable visual models from natural language supervision,” in *International conference on machine learning*. PMLR, 2021, pp. 8748–8763.

[5] X. Zhou, R. Girdhar, A. Joulin, P. Krähenbühl, and I. Misra, “Detecting twenty-thousand classes using image-level supervision,” in *Computer Vision—ECCV 2022: 17th European Conference, Tel Aviv, Israel, October 23–27, 2022, Proceedings, Part IX*. Springer, 2022, pp. 350–368.

[6] M. Wang, J. Xing, and Y. Liu, “Actionclip: A new paradigm for video action recognition,” *arXiv preprint arXiv:2109.08472*, 2021.

[7] B. Feuer, A. Joshi, M. Cho, K. Jani, S. Chiranjeevi, Z. K. Deng, A. Balu, A. K. Singh, S. Sarkar, N. Merchant, A. Singh, B. Ganapathysubramanian, and C. Hegde, “Zero-shot insect detection via weak language supervision,” in *2nd AAAI Workshop on AI for Agriculture and Food Systems*, 2023. [Online]. Available: <https://openreview.net/forum?id=VPDKe672pv>

[8] A. Sanghi, H. Chu, J. G. Lambourne, Y. Wang, C. Cheng, M. Fumero, and K. Malekshan, “Clip-forge: Towards zero-shot text-to-shape generation,” in *2022 IEEE/CVF Conference on Computer Vision and Pattern Recognition (CVPR)*. Los Alamitos, CA, USA: IEEE Computer Society, jun 2022, pp. 18 582–18 592.

[9] A. Jain, B. Mildenhall, J. T. Barron, P. Abbeel, and B. Poole, “Zero-shot text-guided object generation with dream fields,” 2022.

- [10] H. Xu, G. Ghosh, P.-Y. Huang, D. Okhonko, A. Aghajanyan, F. Metzger, L. Zettlemoyer, and C. Feichtenhofer, "VideoCLIP: Contrastive pre-training for zero-shot video-text understanding," in *Proceedings of the 2021 Conference on Empirical Methods in Natural Language Processing (EMNLP)*. Online: Association for Computational Linguistics, Nov. 2021.
- [11] H. Fang, P. Xiong, L. Xu, and Y. Chen, "Clip2video: Mastering video-text retrieval via image clip," *arXiv preprint arXiv:2106.11097*, 2021.
- [12] P. Dollár, V. Rabaud, G. Cottrell, and S. Belongie, "Behavior recognition via sparse spatio-temporal features," in *2005 IEEE International Workshop on Visual Surveillance and Performance Evaluation of Tracking and Surveillance*, 2005, pp. 65–72.
- [13] H. Wang and C. Schmid, "Action recognition with improved trajectories," in *2013 IEEE International Conference on Computer Vision*, 2013, pp. 3551–3558.
- [14] H. Wang, A. Kläser, C. Schmid, and C.-L. Liu, "Dense trajectories and motion boundary descriptors for action recognition," *International journal of computer vision*, vol. 103, no. 1, pp. 60–79, 2013.
- [15] H. Wang and C. Schmid, "Action recognition with improved trajectories," in *2013 IEEE International Conference on Computer Vision*, 2013, pp. 3551–3558.
- [16] K. Simonyan and A. Zisserman, "Very deep convolutional networks for large-scale image recognition," in *International Conference on Learning Representations*, 2015.
- [17] C. Feichtenhofer, H. Fan, J. Malik, and K. He, "Slowfast networks for video recognition," in *Proceedings of the IEEE/CVF international conference on computer vision*, 2019, pp. 6202–6211.
- [18] X. Shi, S. Shan, M. Kan, S. Wu, and X. Chen, "Real-time rotation-invariant face detection with progressive calibration networks," in *Proceedings of the IEEE Conference on Computer Vision and Pattern Recognition*, 2018, pp. 2295–2303.
- [19] N. Kose, O. Kopuklu, A. Unnervik, and G. Rigoll, "Real-time driver state monitoring using a cnn based spatio-temporal approach," in *2019 IEEE Intelligent Transportation Systems Conference (ITSC)*. IEEE, 2019, pp. 3236–3242.
- [20] P. Li, M. Lu, Z. Zhang, D. Shan, and Y. Yang, "A novel spatial-temporal graph for skeleton-based driver action recognition," in *2019 IEEE Intelligent Transportation Systems Conference (ITSC)*. IEEE, 2019, pp. 3243–3248.
- [21] A. Diba, M. Fayyaz, V. Sharma, M. M. Arzani, R. Yousefzadeh, J. Gall, and L. Van Gool, "Spatio-temporal channel correlation networks for action classification," in *Proceedings of the European Conference on Computer Vision (ECCV)*, 2018, pp. 284–299.
- [22] J. Stroud, D. Ross, C. Sun, J. Deng, and R. Sukthankar, "D3d: Distilled 3d networks for video action recognition," in *Proceedings of the IEEE/CVF Winter Conference on Applications of Computer Vision*, 2020, pp. 625–634.
- [23] Y. Abouelnaga, H. M. Eraqi, and M. N. Moustafa, "Real-time distracted driver posture classification," *arXiv preprint arXiv:1706.09498*, 2017.
- [24] C. Huang, X. Wang, J. Cao, S. Wang, and Y. Zhang, "Hcf: a hybrid cnn framework for behavior detection of distracted drivers," *IEEE access*, vol. 8, pp. 109 335–109 349, 2020.
- [25] K. He, X. Zhang, S. Ren, and J. Sun, "Deep residual learning for image recognition," in *Proceedings of the IEEE conference on computer vision and pattern recognition*, 2016, pp. 770–778.
- [26] F. Chollet, "Xception: Deep learning with depthwise separable convolutions," in *2017 IEEE Conference on Computer Vision and Pattern Recognition (CVPR)*, 2017, pp. 1800–1807.
- [27] C. Szegedy, V. Vanhoucke, S. Ioffe, J. Shlens, and Z. Wojna, "Rethinking the inception architecture for computer vision," in *2016 IEEE Conference on Computer Vision and Pattern Recognition (CVPR)*, 2016, pp. 2818–2826.
- [28] J. Carreira and A. Zisserman, "Quo vadis, action recognition? a new model and the kinetics dataset," in *proceedings of the IEEE Conference on Computer Vision and Pattern Recognition*, 2017, pp. 6299–6308.
- [29] K. Simonyan and A. Zisserman, "Two-stream convolutional networks for action recognition in videos," *Advances in neural information processing systems*, vol. 27, 2014.
- [30] C. Feichtenhofer, A. Pinz, and A. Zisserman, "Convolutional two-stream network fusion for video action recognition," in *Proceedings of the IEEE conference on Computer Vision and Pattern Recognition*, 2016, pp. 1933–1941.
- [31] A. Arnab, M. Dehghani, G. Heigold, C. Sun, M. Lucic, and C. Schmid, "Vivit: A video vision transformer," in *2021 IEEE/CVF International Conference on Computer Vision (ICCV)*. Los Alamitos, CA, USA: IEEE Computer Society, oct 2021, pp. 6816–6826.
- [32] H. Fan, B. Xiong, K. Mangalam, Y. Li, Z. Yan, J. Malik, and C. Feichtenhofer, "Multiscale vision transformers," in *Proceedings of the IEEE/CVF International Conference on Computer Vision*, 2021, pp. 6824–6835.
- [33] G. Bertasius, H. Wang, and L. Torresani, "Is space-time attention all you need for video understanding?" in *ICML*, vol. 2, no. 3, 2021, p. 4.
- [34] A. Miech, D. Zhukov, J.-B. Alayrac, M. Tapaswi, I. Laptev, and J. Sivic, "Howto100m: Learning a text-video embedding by watching hundred million narrated video clips," in *Proceedings of the IEEE/CVF International Conference on Computer Vision*, 2019, pp. 2630–2640.
- [35] N. C. Miithun, R. Panda, E. E. Papalexakis, and A. K. Roy-Chowdhury, "Webly supervised joint embedding for cross-modal image-text retrieval," in *Proceedings of the 26th ACM international conference on Multimedia*, 2018, pp. 1856–1864.
- [36] J. Dong, X. Li, C. Xu, S. Ji, Y. He, G. Yang, and X. Wang, "Dual encoding for zero-example video retrieval," in *Proceedings of the IEEE/CVF conference on computer vision and pattern recognition*, 2019, pp. 9346–9355.
- [37] S. Xie, C. Sun, J. Huang, Z. Tu, and K. Murphy, "Rethinking spatiotemporal feature learning: Speed-accuracy trade-offs in video classification," in *Proceedings of the European conference on computer vision (ECCV)*, 2018, pp. 305–321.
- [38] M. S. Rahman, A. Venkatachalapathy, A. Sharma, J. Wang, S. V. Gursoy, D. Anastasiu, and S. Wang, "Synthetic distracted driving (syndd1) dataset for analyzing distracted behaviors and various gaze zones of a driver," *Data in Brief*, vol. 46, p. 108793, 2023. [Online]. Available: <https://www.sciencedirect.com/science/article/pii/S2352340922009969>
- [39] "Kaggle. state farm distracted driver detection." [Online]. Available: <https://www.kaggle.com/competitions/state-farm-distracted-driver-detection/data>
- [40] A. Miech, J.-B. Alayrac, L. Smaira, I. Laptev, J. Sivic, and A. Zisserman, "End-to-end learning of visual representations from uncurated instructional videos," in *Proceedings of the IEEE/CVF Conference on Computer Vision and Pattern Recognition*, 2020, pp. 9879–9889.
- [41] D. P. Kingma and J. Ba, "Adam: A method for stochastic optimization," *arXiv preprint arXiv:1412.6980*, 2014.
- [42] A. Krizhevsky, I. Sutskever, and G. E. Hinton, "Imagenet classification with deep convolutional neural networks," *Communications of the ACM*, vol. 60, no. 6, pp. 84–90, 2017.
- [43] M. Sandler, A. Howard, M. Zhu, A. Zhmoginov, and L.-C. Chen, "Mobilenetv2: Inverted residuals and linear bottlenecks," in *Proceedings of the IEEE conference on computer vision and pattern recognition*, 2018, pp. 4510–4520.



**Md Zahid Hasan** received his B.S. degree in Electrical and Electronic Engineering from Bangladesh University of Engineering and Technology in 2018. He is currently pursuing his Ph.D. in Electrical Engineering with the Department of Electrical and Computer Engineering at Iowa State University, IA. His research interests include Vision-Language models, computer vision, machine learning and decentralized deep learning.



**Jiajing Chen** received the B.S. degree in mechanical engineering from Wuhan Institute of Technology, Wuhan, China in 2017 and M.S. degree in mechanical engineering from Syracuse University, Syracuse, NY, USA in 2019. He is currently pursuing the Ph.D. degree with the Department of Electrical Engineering and Computer Science, Syracuse University. His research interests include Point Cloud Segmentation, Weakly Supervised Object Detection and Few-shot Learning.



**Jiyang Wang** received his Bachelor's degree in electrical engineering from Anhui University of Science and Technology in 2017 and a Master's degree in electrical engineering from Syracuse University in 2019. He is currently a Ph.D. student in Electrical and Computer Engineering at Syracuse University. His research interests include computer vision, deep learning and human computer interaction.



**Ameya Joshi** received his B.S. degree in Electrical and Electronics Engineering from BITS Pilani, Goa, India in 2014. He is currently pursuing his Ph.D. in Electrical Engineering with the Department of Electrical and Computer Engineering at New York University. He was previously a Ph.D. student at Iowa State University (2018-2019) before going to NYU. His research interests include robust algorithms for multimodal models, adversarial robustness for deep learning, Vision-Text models, generative models for structured data, Physics Informed Generative models, Generative Adversarial Networks and computer vision.

generative models, Generative Adversarial Networks and computer vision.



**Senem Velipasalar** (M'04-SM'14) received the Ph.D. and M.A degrees in electrical engineering from Princeton University, Princeton, NJ, USA, in 2007 and 2004, respectively, the M.S. degree in electrical sciences and computer engineering from Brown University, Providence, RI, USA, in 2001, and the B.S. degree in electrical and electronic engineering from Bogazici University, Istanbul, Turkey, in 1999. From 2007 to 2011, she was an Assistant Professor at the Department of Electrical Engineering, University of Nebraska-Lincoln. She is currently

a Professor in the Department of Electrical Engineering and Computer Science, Syracuse University. The focus of her research has been on machine learning, mobile camera applications, wireless embedded smart cameras, multicamera tracking and surveillance systems.



**Chinmay Hegde** received his Ph.D. and M.S. in Electrical and Computer Engineering from Rice University in 2012 and 2010 respectively. He joined New York University, Tandon School of Engineering as an Assistant Professor in 2019. Previously, he was an Assistant Professor in the Department of Electrical and Computer Engineering at Iowa State University from 2015 to 2019. Prior to joining Iowa State, he was a postdoctoral associate in the Theory of Computation group at MIT from 2012 to 2015. His research focuses on developing principled, fast,

and robust algorithms for diverse problems in machine learning, with applications to imaging and computer vision, materials design and transportation.



**Anuj Sharma** received his Ph.D. degree in Civil Engineering from Purdue University in 2008, and his M.S. degree in Civil Engineering from Texas A&M University in 2004. He was an Assistant Professor in the Department of Civil Engineering at the University of Nebraska-Lincoln. He is currently a Pitts-Des Moines Inc. Professor in Civil Engineering at Iowa State University. His research focuses on traffic operations, big data analytics, machine learning, and traffic safety.



**Soumik Sarkar** received his Ph.D. in Mechanical Engineering from Penn State University in 2011. He joined the Department of Mechanical Engineering at Iowa State as an Assistant Professor in Fall 2014. Previously, he was with the Decision Support and Machine Intelligence group at the United Technologies Research Center for 3 years as a Senior Scientist. He is currently a Professor of Mechanical Engineering and Walter W Wilson Faculty Fellow in Engineering at Iowa State University. He also serves as the Director of Translational AI Center

at Iowa State. His research focuses on machine learning, and controls for Cyber-Physical Systems applications such as aerospace, energy, transportation, manufacturing and agricultural systems.